Available online at www.sciencedirect.com

jmr&t Journal of Materials Research and Technology

journal homepage: www.elsevier.com/locate/jmrt

Original Article

Synergistic effects of tubular halloysite clay and zirconium phosphate on thermal behavior of intumescent coating for structural steel

Yuan Xien Lee [a], Faiz Ahmad [a,*], Sarower Kabir [a], Patrick J. Masset [b], Eugenio Onate [c], Guan Heng Yeoh [d]

[a] Department of Mechanical Engineering, Universiti Teknologi PETRONAS, 32610 Bandar Seri Iskandar, Perak Malaysia
[b] Technallium Engineering & Consulting, Fliederweg 6, D-92449 Steinerg Am See, Germany
[c] International Centre for Numerical Methods in Engineering (CIMNE), Universitat Politècnica de Catalunya (UPC), Barcelona, Spain
[d] Mechanical Engineering, University of New South Wales, Kensington, New South Wales, Australia

ARTICLE INFO

Article history:
Received 20 December 2021
Accepted 20 April 2022
Available online 25 April 2022

Keywords:
Intumescent fire protective coating
Synergy
Tubular halloysite clay (THC)
Zirconium phosphate (ZrP)
Water resistance
XPS analysis

ABSTRACT

Zirconium phosphate (ZrP) recently introduced in intumescent fire protective coating has shown improvement in developing ceramic layer. The tubular halloysite clay (THC) due to its unique molecular structure can be combined with ZrP to enhance fire resistance by developing a strong silica network on the char surface. This study is aimed to investigate the synergistic effects of tubular halloysite clay and zirconium phosphate fillers to improve the thermal performance of the intumescent coating. The control coating formulation and a range of coating formulations using a combination of weight percentage of THC and ZrP were developed to study the influences of fillers on fire performance. The char expansion and fire resistance tests of the coatings were conducted using furnace fire test and Lab scale fire jet. Thermal stability of the coating was determined by TGA and char was characterized by FESEM, XRD, FTIR and XPS. Water-resistance test of the coating was performed according to ASTM D-870. Results showed that the reinforcement of THC-ZrP showed promising improvement on the performance of IFC and substrate temperature was far below the critical temperature, 550 °C. Sample HZ 5 showed the least backside steel substrate temperature of 219 °C. Expansion rate of char was found reduced with the addition of THC but improved the char compactness. The addition of THC and ZrP in IFC improved 18% fire resistance performance and 5% residual wt. Of char. Char morphology showed silica network, XRD and FTIR confirmed the presence of silicon. Water absorption test showed 95% less water absorption (HZ-5) compared to control coating. Post water immersion, fire test showed 7% increase in substrate temperature which is 18% less than control coating after water immersion fire test.

* Corresponding author.
E-mail addresses: faizahmad@utp.edu.my, faizahmadster@gmail.com (F. Ahmad).
https://doi.org/10.1016/j.jmrt.2022.04.097

1. Introduction

Steel being a high strength material, is an essential element of construction industry, however, in the event of fire, it loses 50% of its load bearing capability when temperature exceed its critical temperature of 500 °C, and building will collapse in less than an hour. In such circumstances, the safety of individuals and assets against fire is undoubtedly a challenge. The passive fire protective systems are in practice [1,2] for fire protection of buildings, but the performance of these systems against fire has been a great challenge. This system is a mixture of fire-resistant components that increases the resistance to flammability. In 90's, halogenated compounds in a combination of epoxy were popular flame retardants. However, these fire protectives release harmful compounds to the environment during degradation [5,6]. Recent regulations have been introduced to restrict the application of toxic compounds. In the buildings, the new flame retardants are introduced to substitute their halogenated counterparts [7,8].

Intumescent fire protective coatings consist of a resin binder blended with fire protective intumescent system. Typically, three active ingredients are used in the intumescent system: an acid source, a carbon source, and a blowing agent. The homogenous mixture of these ingredients expands coherently on exposure to the heat source and form a cellular insulative foam to resist the fire penetration to substrate. One of the major advantage of intumescent fire protective coatings is the ease in their application over a wide range of substrates [1–4] without affecting their bulk properties [5,6]. In addition to reducing the inflammability of the substrate, these coatings decrease the heat transfer from the fire to the substrate and able to maintain the substrate temperature below the critical temperature (e.g., 550 °C for steels) for few hrs. even the flame temperature reaches to 1000 °C [1]. It was reported in the literature that steel structures might collapse within less than 45 min when its temperature rises above 550 °C [7]. The traditional intumescent coating system typically comprises of ammonium polyphosphate (APP) as a source of acid, pentaerythritol as a source of carbon and melamine (MEL) as a blowing material. Expandable graphite (EG) has been used to increase the anti-oxidant properties as a synergistic component [8,9].

The exceptional chemical properties, thermal stability and highly catalytic qualities of mineral fillers exhibit promising flame retardant properties for polymers [10]. Lu et al. [11] conducted an experiment to investigate the influence of polystyrene and poly(ethylene-co-vinyl acetate) with organically modified zirconium phosphate (OZrP) by melt blending. They confirmed the addition of OZrP increased thermal stability at high temperature and slightly reduce the peak heat release rate through cone calorimetry analysis. Through TGA, they found out the char left was increasing with the weightage of OZrP where the 5% of OZrP has the highest char left with 2.5%. Weiyi Xing et al. [12] evaluated the effect of ZrP on the thermal degradation and flame retardation of the coating. Microscale combustion calorimeter (MCC) tests showed a substantial decrease in heat release intensity and overall combustion heat of coatings reinforced with ZrP and a noticeable increase in the char yield. The addition of 0.5 mass % ZrP, resulted in maximum fire protective performance. XPS study revealed that the incorporation of ZrP increased the anti-oxidation efficiency of the coating. Yong Luo et al. [13] investigated the flame retardancy of PVA aerogels which was strengthened by APP and a-ZrP. The inclusion of a-ZrP enhanced the 3D network configuration of the PVA aerogel. Thermogravimetric Analysis (TGA) showed that a-ZrP favored the PVA-APP system's thermal stability. Residues analysis indicated that a-ZrP facilitated the creation of a compact graphite structure and catalyzed the PVA charring during combustion. In recent years, filler-based polymer composites revolutionize the flame-retardant sector, offering significant benefits over traditional coatings. The study was focused to use silicate for manufacturing coating materials with enhanced flame retardant properties [14,15]. However, using silicate compounds alone was not improving the fire resistance compared to the use of filler based polymer composites in colligation with conventional flame retardants [16]. Tubular Halloysite clay ($Al_2Si_2O_5$ $(OH)_4.2H_2O$), a potential filler was reported to strengthen the fire resistance performance [17,18]. High aspect ratio and mechanical strength make THC's superior to CNT's [19]. Latest studies reported that THC's have a positive effect on epoxy-based intumescent fire protective coating [20]. On the other hand, zirconium phosphate was reported as a filler to enhance the flame retardancy due to its excellent chemical properties and thermal stability [21]. Therefore, synergistic effects of both THC and ZrP reinforced fillers are promising to evaluate as no study was conducted yet.

In this research work formulations using THC and ZrP reinforced epoxy based intumescent coating were developed and investigated to analyze the combined effects of reinforcement on the performance of the coating system. The coatings were evaluated for their fire resistance using lab scale fire jet test, char expansion, char morphology, thermal degradation analysis, XRD, FTIR, XPS, water absorption behavior of coatings and post water immersion, fire resistance performance.

2. Materials and methods

2.1. *Coating materials*

Zirconium phosphate powder was purchased from Sichuan Hongchang Plastics Indus. Co. Ltd. China. Expandable graphite, boric acid, ammonium polyphosphate, melamine and tubular halloysite clay were purchased from Sigma Aldrich (M) Sdn Bhd. Malaysia. BE-188 (BPA) resin and H-2310 polyamide amine were used as a binder and brought from Mc-Growth Chemical Sdn Bhd. Malaysia. TSA Industries, Ipoh Sdn Bhd, Malaysia supplied structural steel A36. The thickness of steel plates was 1.50 mm ± 0.05. SEM test was conducted to

analyze the orientation of tubular halloysite clay and zirconium phosphate used in this study and presented in Fig. 1.

2.2. Coating preparation

Control formulation without any filler were developed. To determine the ratio of THC or ZrP, formulation containing 0.1wt% of THC and 0.1wt% of ZrP was done to examine the char structure. Physical examination of char showed that char of ZrP reinforced coating exhibit cracks and uneven surface. The char of THC reinforced coating was uniform, and cracks were reduced, as shown in Fig. 2. These results motivated to investigate the synergistic effects of THC and ZrP to improve the overall quality of the coating formulations studied and influence of resulting char on improvement of fire resistance.

To prepare the coatings, ammonium polyphosphate (APP), boric acid (BA), melamine (MEL) and tubular halloysite clay (THC) and zirconium phosphate was accurately weighed (Table 1) using weighing balance and were homogenized using blender mixer for 90s without expandable graphite. To ensure homogeneous mixture of fire-resistant ingredients, EG was dispersed in the mixture manually to avoid mechanical damage to its particles. Mixture was then stirred with a stirring rod for 5 min and the mixture was considered ready for dispersion in epoxy and hardener to develop coatings. The mass percentage of reinforcement, THC and ZrP was maintained to one and ratio of THC-ZrP was changed to study their influence on thermal degradation and fire-resistant performance. This mass percentage was substituted for binder percentage to maintain epoxy to hardener ration 2:1. The ingredients of control formulations, HZ-0 was selected based on our earlier study [22] and was used to assess the comparison in improvement in performance of THC and ZrP reinforced coating formulations. The ingredient mixture was slowly added with epoxy (BE-188) under continuous stirring at 40 rpm for 15 min using an automatic shear mixer CAFRAMO (BDC 6015-220). To finalize the coating, the hardener (H-2310) was added and stirred for another 10 min at 60 rpm. After ensuring a homogeneous mixing of coating, it was ready for application on substrate.

Steel substrate with dimension 10 × 10 cm^2 was sand-blasted. Coating was then applied on steel plates with the help of a brush to ensure uniformly thickness on the substrate leaving no corner uncoated. An average thickness of the coating 1.0–1.50 mm was maintained. The samples were kept at the ambient temperature for 1 day for curing, and environment humidity was about 80%.

3. Characterization of intumescent coating and char

3.1. Furnace fire test

The thickness of the dried or cured coatings was measured using a digital Vernier caliper. The coated steel substrates were then burnt at 500 °C in a carbolite furnace (model no. RWF 11/13 having a temperature range of 30–1300 °C) to examine the influence of reinforcement of char expansion, physical appearance, and its adhesion with the substrate. The heating rate was set at 20 °C/min and temperature reached to 500 °C in 25 min. This temperature was maintained for 1 h to ensure complete degradation of coating ingredients and complete expansion [23]. The samples were cooled in the furnace to 25 °C to avoid thermal cracking of the chars due to temperature variation with the external environment. The char expansion for each formulation was measured using a digital Vernier caliper, and an average of 4 measurements is reported.

3.2. Laboratory scale jet fire test

To measure the heat incursion on the steel plate during the fire test, lab scale jet fire test using Bunsen burner was conducted according to ASTM E-119. A portable premium butane gas having gas flow rate of 105 g/h was used to test the heat penetration on coated steel samples. During this test, 7 cm distance was maintained between the coated steel substrates and the burner. The substrate backside temperature was recorded using Three K-type tthermocouples' attached at the

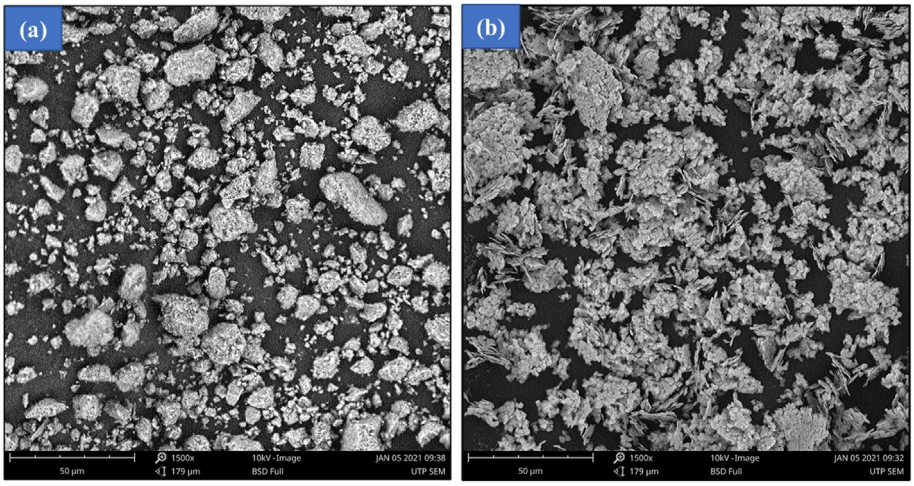

Fig. 1 – SEM micrograph of (a) THC and (b) ZrP used in this study.

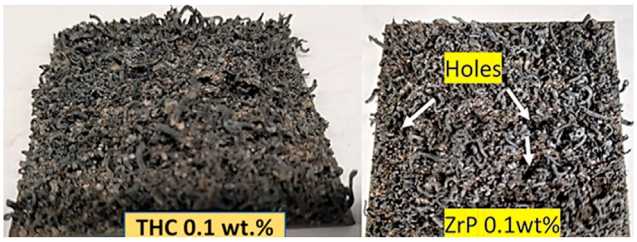

Fig. 2 – Physical appearance of coating char of THC 0.1wt% and ZrP 0.1wt%.

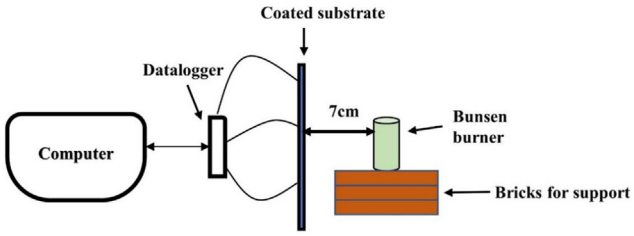

Fig. 3 – Schematic diagram of the laboratory scale jet fire test.

backside of the coated substrates with the help of X'traseal 650°F Red RTV Silicon glue (Fig. 3). The change in substrate temperature was recorded using a data logger interfaced with PC for 1 h at 30 s interval.

3.3. *Thermogravimetric analysis (TGA)*

TGA was used to determine the influence of reinforced THC and ZrP on degradation of coating samples and to evaluate the changes in residual mass of the char. 10 mg of coating sample was heated in a crucible at 10 °C/min under nitrogen in the 25-800 °C temperature range using Q50 Perkin Elmer thermal analyzer.

3.4. *X-ray diffraction analysis (XRD)*

XRD was performed to examine the phases of compounds in the residue char samples after the furnace test. 2–3g of char sample was used in this testing for analysis of char. A Diffractometer Bruker AXS D8 Advance using Cu and Kα radiation with a nickel filter ($\lambda = 0.150595$ mm) in range ($10 < 2\Theta < 90$).

3.5. *Fourier transform infrared spectroscopy (FTIR) analysis*

Approximately 2 gm of char sample was used to determine the presence of degradation compounds in the char. A EQUINOX55 FTIR spectrometer was used to record the FTIR spectra in the 4000 cm^{-1} to 400 cm^{-1} range using KBr pellet technology.

3.6. *Field emission scanning electron microscopy (FESEM)*

Char morphology was analyzed using FESEM model SUPRA 55VP. Magnification was varied from 50X to 2000X. A fully developed char of each sample was used to examine the morphology of the char after the furnace test.

3.7. *X-ray photoelectron spectroscopy analysis (XPS)*

The elemental composition of the char sample of the coating and presence of possible compounds in the char were investigated by XPS analysis using an XPS model LEYBOLD spectrometer. The Al Kα radiation was used and run in a fixed analyzer transmission mode at the pass energy of 50 eV. Char samples were mounted by pressing onto the indium holder and introduced in a pre-chamber to obtain a pressure of 10^{-5} Torr.

3.8. *Water resistance test*

Water-resistance test was performed according to ASTM D870. An ultra-sonic cleaner filled with distilled water was used to clean the surface of coating samples [24] and dried with hot air to ensure clean surface before measuring their weight. After immersion of test samples in distilled water, the weight of samples was recorded after every 24 h for 14 days. The results presented are the average of three measurements. The mass change rate (R%) was calculated using the following Eq. (1) [25].

$$R\ (\%) = \left(\frac{m_2 - m_1}{m_1}\right) \times 100 \quad (1)$$

where m_1 and m_2 correspond to the masses of the coated samples before and after the test, respectively.

4. Results and discussions

4.1. *Physical appearance of char and intumescent factor*

The pictures of coated samples before and after the furnace fire test are shown in Fig. 4. The coated samples showed

Table 1 – Mass percentage of intumescent ingredients used to develop coating formulations.

Sample	APP	MEL	BA	EG	THC	ZrP	Epoxy Resin	Hardener
HZ-0	11.36	5.5	11	5.5	–	–	44.44	22.22
HZ-1	11.36	5.5	11	5.5	0.1	0.9	43.94	21.72
HZ-2	11.36	5.5	11	5.5	0.2	0.8	43.94	21.72
HZ-3	11.36	5.5	11	5.5	0.3	0.7	43.94	21.72
HZ-4	11.36	5.5	11	5.5	0.4	0.6	43.94	21.72
HZ-5	11.36	5.5	11	5.5	0.5	0.5	43.94	21.72

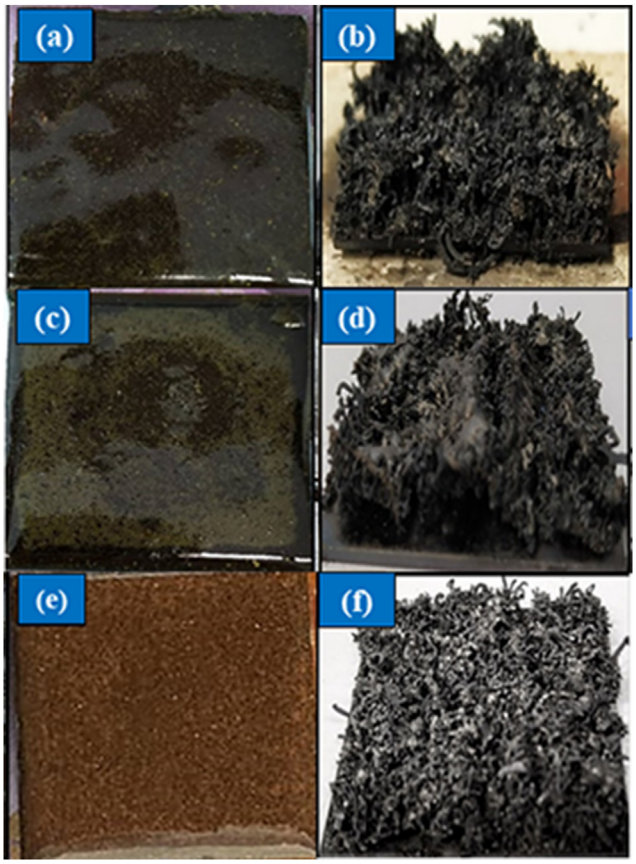

Fig. 4 – Coated steel samples before furnace test (a) HZ0 (c) HZ1 (e) HZ5 and char samples after furnace test (b) HZ0 (d) HZ1 (f) HZ5.

changes in color of the coating from dark green to brownish with decrease in ratio of ZrP in the formulation. After the coated samples underwent furnace test, the improvement in the char' structure was observed with inclusion of both fillers. The char of coating reinforced with fillers appeared to be more homogenous, compact, and white oxidative layer on the surface, as shown in Fig. 4d, f. The char expansion of coating formulations was evaluated by calculating intumescent factor. The char expansion result showed that the fillers improved physical structure of the char as compared to the reference sample (HZ0). It was noted that char of HZ1 was partially detached from the substrate, whereas HZ2 was completely detached. Cracks and tiny uniform holes were observed in the char of HZ3, but the tinny holed structure was also noted for HZ4. HZ5 exhibited a uniform char without crack or micro-sized holes throughout the char. The intumescent factor (IF) for char of each formulation was calculated using formula 2 [26] and presented in Fig. 5.

$$IF = \frac{(d_2 - d_o)}{(d_1 - d_o)} \quad (2)$$

where d_o is the thickness of the substrate, d_1 is the thickness of coating including the substrate and d_2 is final expansion of char, after the furnace test, respectively.

Fig. 5 depicts the reduction in char expansion in terms of intumescent factor. It was observed that the addition of fillers

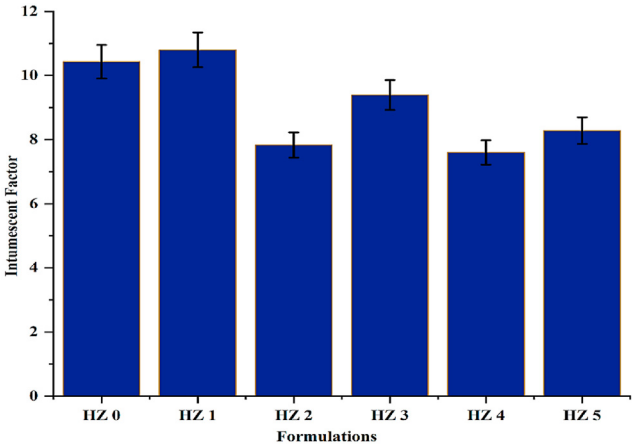

Fig. 5 – Intumescent factor of THC-Zirconium Phosphate reinforced IFRC samples.

in coating formulations, decreased char expansion. The values for IF for formulations HZ0, HZ1, HZ2, HZ3, HZ4 and HZ5 were 10.43, 10.80, 7.83, 9.39, 7.60 and 8.28, respectively. The maximum reduction in char expansion recoded was 27.13% for HZ-4 compared to control formulation, while maximum char expansion was observed in HZ1 which has 0.1 mass percent THC and 0.9 mass percent ZrP. THC has hollow tubular structure and thermally stable a high temperature due to their atomic arrangement. There is possibility that THC may trap non-combustible gases in the hollow tubular structure which not only help in crosslinking but also increase compactness of char [25]. As the THC percentage was increase, evolved gases may be trapped within THC, resulting more compact char thus reducing expansion. Less percentage of THC may have lower resistance to escape the gases causing expansion of char due to presence of ZrP. ZrP hold catalytic charring and dehydration agent in the coating [27], while THC helped to develop the cross-linking network and constrict the expansion of char. 0.1% THC with 0.9%ZrP (HZ 1) increased the char expansion approximately 1.2% compared to HZ0 showing that ZrP is contributing in char forming. It was noted that with the percentage of ZrP in the formulation, the char expansion is decreasing. An increase in percentage of THC in HZ1-HZ5 formulations enhanced char compactness, developing a strong crosslinking and dehydration during the degradation of coating. The presence of THC in coating formulation, in addition of cross-linking, helps to develop ceramic like layer on the char surface reducing the escape of gases and resulting a relatively compact char.

4.2. *Analysis of fire resistance of THC-ZrP reinforced intumescent coating*

Fire resistance performance of the coated samples was evaluated through a laboratory scale jet fire test according to ASTM E-119 standardized procedure. The temperature profiles of all coating samples studied displayed a similar drift. During the first 5 min of test, the significant rise in substrate temperature suggests that the early degradation of the coating ingredients led to develop a multi-porous intumescent layer of the char and substrate temperature was less than 200 °C.

Transient temperature behavior pattern was similar for all the coating samples. From Fig. 6, the reference sample (HZ-0) has a backside temperature of 270 °C after 60 min exposure to fire, which is the highest among all samples studied. Usually, the temperature of the unprotected steel substrate increases in first 10 min and reaches to 500 °C. However similar tendency was also noticed among samples reinforced with fillers but after 30 min, the temperature of the samples other than HZ 0 started decreasing as the fillers started degrading and swell. Reference sample (HZ-0) rises in temperature after 30 min due to scatter of fragile char under pressure of direct fire. The temperature reduction of 18% was recorded for HZ-5 (0.5% of THC and 0.5% of ZrP), which is the best result among the studied formulations. This result due to good dispersion of THC in the coating and balanced mass percentage of THC/ZrP. The substrate backside temperatures of HZ-1, HZ-2 HZ-3 and HZ-4 were 229 °C, 227.9 °C, 225.2 °C and 224.2 °C respectively. Ullah et al. [28] stated that after 60 min fire test, 257 °C temperature of the substrate was recorded for intumescent coating reinforced with 5% kaolin clay. This study showed that reinforcement of both THC and ZrP improved the fire-resistant characteristics of the epoxy-based coating system and showed that there are some synergies between ZrP and THCs in terms of dispersion of THC and influence of ZrP on degradation of coating, as noted during TGA tests.

Although the minor changes in the temperature were recorded for coated substrates during thermal resistance test. The minor changes may be considered due to the experimental error. The test conducted in a chamber has influence of air cooling on the substrate. Nevertheless, the substrate temperature for coating decreases as the ratio of THCs and ZrP content approaches to 0.5:0.5. It was considered that the percentage of THCs can help to crosslink the carbon atoms and forms high-density bridge linkages among the char. Concurrently, ZrP-degrades to non-combustible gasses that can decrease the stability of the charring mechanism and fracture the extended carbon layer. Consequently, the shield created by the carbon layer is reduced, therefore decreasing the flame resistance of the coating.

The degradation of epoxy and intumescent ingredients helps to develop crosslinking by THC with the carbon atoms and increase the char compactness. While non-combustible gases such as (phosphorus oxide) produced by pyrolysis of ZrP tends to fracture the carbon network thus producing a soft char that made minor increase in substrate temperature [12]. This was recorded for formulations containing higher percentage of ZrP.

Based on the findings, a possible mechanism is proposed to describe the synergistic activity between THCs, ZrP, ammonium polyphosphate (APP), melamine (MEL), Boric acid (BA), expandable graphite (EG) and epoxy. The early stage in the burning process is the thermal deterioration of APP to the development of polyphosphoric acid (PPA) with the removal of water and ammonia, and the self-crossing linking reaction of minimal PPA [29,30]. Then, phosphate ester bonding degrades into epoxy chains through the dehydration reaction occurred [31]. The intumescent char started to form during the second stage degradation process which started at 220 °C [32]. Besides, ZrP may be integrated as a synergistic agent in the forming of carbonaceous char through organic catalyst reactions. ZrP is assumed to be a multilayer acid catalyst that has either Brønsted (H^+) and Lewis (Zr^{4+}) acidic positions on its surface [33]. During its pyrolysis step, the epoxy chain appears to be catalytically burnt, while boric acid and melamine materials are degraded later. THCs and Zr^{4+} additionally speed up crosslinking cyclization, condensation, dehydrogenation and aromatic reactions, which supports the formulation of an extensive residue of carbon [12,34]. Since the steel substrate used is sand blasted with surface roughness value of Ra 2–2.5. After sand blasting, the surface of steel substrate was un-even and char creates an-interlocking with the substrate surface thus enhancing adhesion of char with substrate [32].

The increase in substrate temperature of HZ1 was considered due to presence of higher percentage of ZrP which is charring catalyst and produced soft char. The soft char was not able to protect the heat penetration to the substrate. The influence of THC (0.1) was negligible in terms of fire protection [25]. The increase in THC percentage reduced the substrate temperature making char more compact.

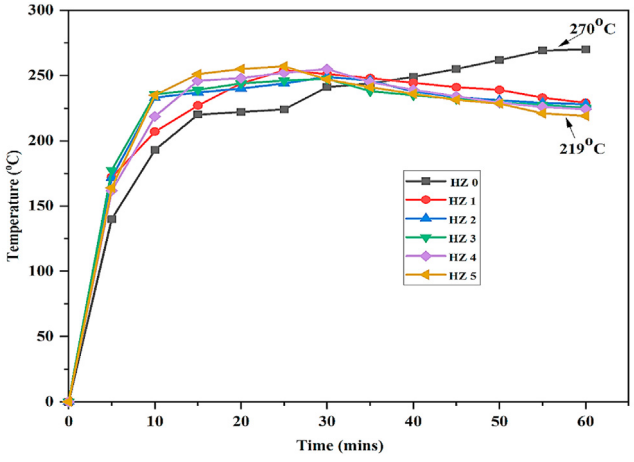

Fig. 6 – Temperature versus time of THC-ZrP reinforced IFRC samples during laboratory scale jet fire tests.

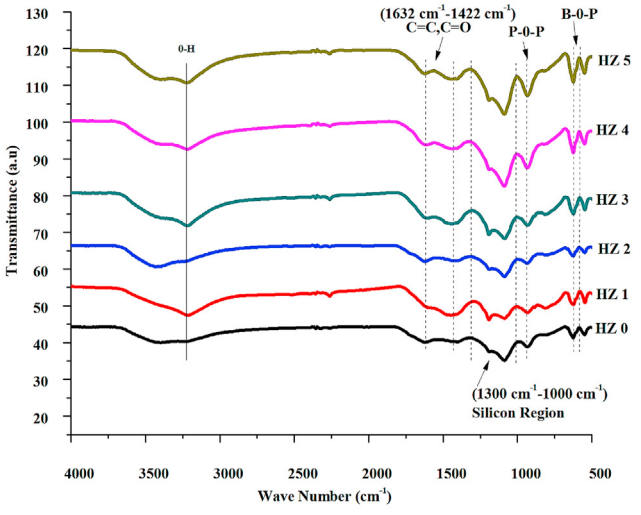

Fig. 7 – FTIR spectra of THC-ZrP reinforced intumescent coatings after furnace tests.

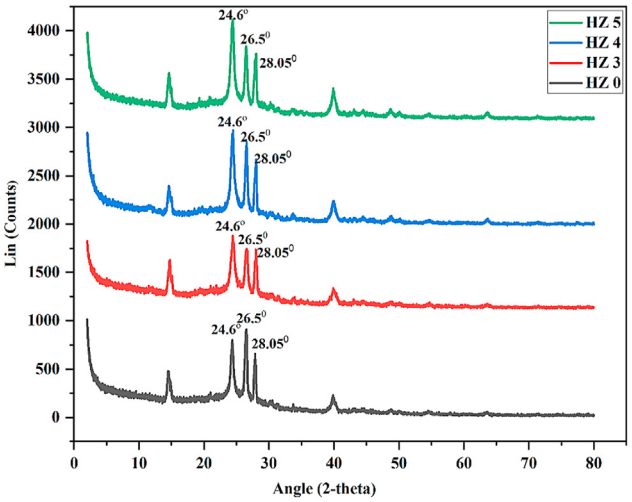

Fig. 8 – XRD spectrum of HZ 0, HZ 3, HZ 4, and HZ 5.

4.3. *FTIR analysis of char*

The analysis of the char offers insight into the efficiency of fire-resistance materials available in the char produced due to the degradation of coating ingredients on exposure to fire. Fig. 7 shows the FTIR spectra of char samples of coating formulations of HZ-0, HZ-1, HZ-2, HZ-3, HZ-4, and HZ-5 after furnace test. FTIR spectrum demonstrating that the reinforcement of ZrP and THC has slight impact on the improvement of thermal degradation performances of the coating formulation compared to Control formulation, HZ-0. Two stretching peaks were found in the 1632 cm^{-1}- 1422 cm^{-1} region which represent the C=C and C = 0 bonding because of the amorphous carbon which comes from amine and graphite functional group respectively (APP and MEL) [31,35]. Recorded peaks in the range 1300 cm^{-1} – 1000 cm^{-1} belong to silicon species [35]. Apart from the reference sample HZ-0, other samples showed peaks ascribed to the bonding stretching of silicon-based species and confirm the presence of silicon in the char samples, indicating the presence of THC in the coating. Two sharp peaks were found (610 and 570 cm^{-1}) that ensures the presence of B-O-P bonding hence the existence of boron phosphate [36,37]. Peaks at 936 cm^{-1} belong to the P-O-P bonding [38]. The presence of hydroxyl group (0-H) was found in the region 3224 cm^{-1}-3239 cm^{-1} arising from the decomposition of epoxy resin [39].

The results of FTIR demonstrated that the presence of functional groups observed in the char led to better resistance to fire at test temperature, 550 °C. The presence of these compounds in the char was due to the reinforcement of THC, and ZrP that has increased the thermal efficiency of the intumescent coatings.

4.4. *Analysis of char composition*

To evaluate the presence of compounds of degraded coating ingredient, X-ray diffraction analysis was carried out. XRD diffraction pattern of samples HZ0, HZ3, HZ4 and HZ5 are shown in Fig. 8. Spectrum behavior appeared was almost symmetrical in THC-ZrP reinforced coatings char in terms of peaks. Sassolite ($H_3B_1O_{3)}$, ICDD reference no. 98-002-4711 was found in its anorthic crystal form at 24.6° (d spacing 3.18). Boron-phosphate (BPO_4), ICDD reference no 01-07 2-9924, was confirmed with a peak at 26.5° (d spacing 3.64). Inorganic, tetragonal boron-phosphate was identified with peaks at 28.81°, 39.54° and 46.18°. Diffraction peak at 28.05° (d spacing 3.17) was assigned to silicate mineral, 'mullite' [40]. Peaks recorded at 43.45° (d spacing 2.08) and 26.60° (d spacing 3.34) was assigned to carbon, ICDD reference no. 00-026-1079 [41]. ZrP was identified with typical diffraction peaks at 11.6° and 19.8° in plate-like structures [42]. Orthorhombic crystal ammonium molybdenum oxide [$(NH_4)_2MO_4O_{13}$], ICDD reference no. 00-050-0608 exhibit two peaks at 11.45° (d spacing 7.49) and 15.02° (d spacing 5.89).

Boric acid is converted successively into meta boric acid and then into boron oxide during decomposition. The XRD findings revealed that the reactions within fillers strengthened coatings antioxidant efficiency by the reinforcement of

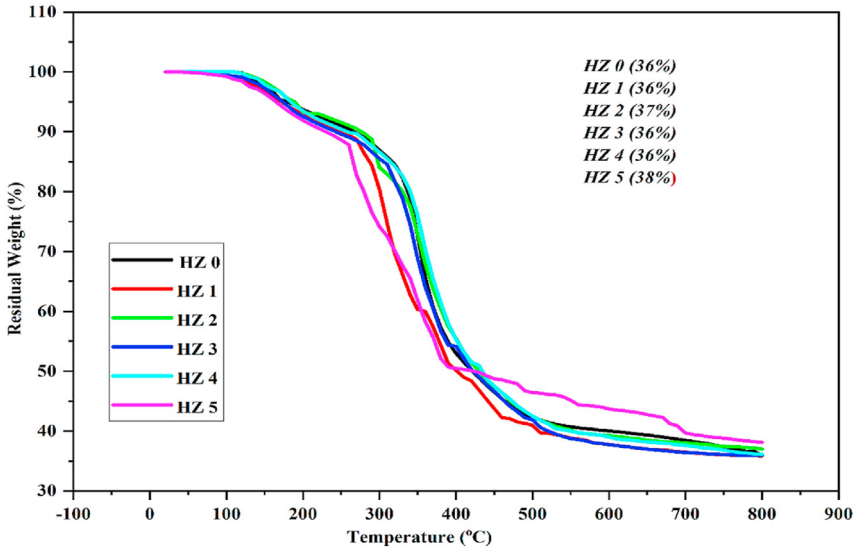

Fig. 9 – Evolution of the sample mass versus the temperature of the 5 investigated samples.

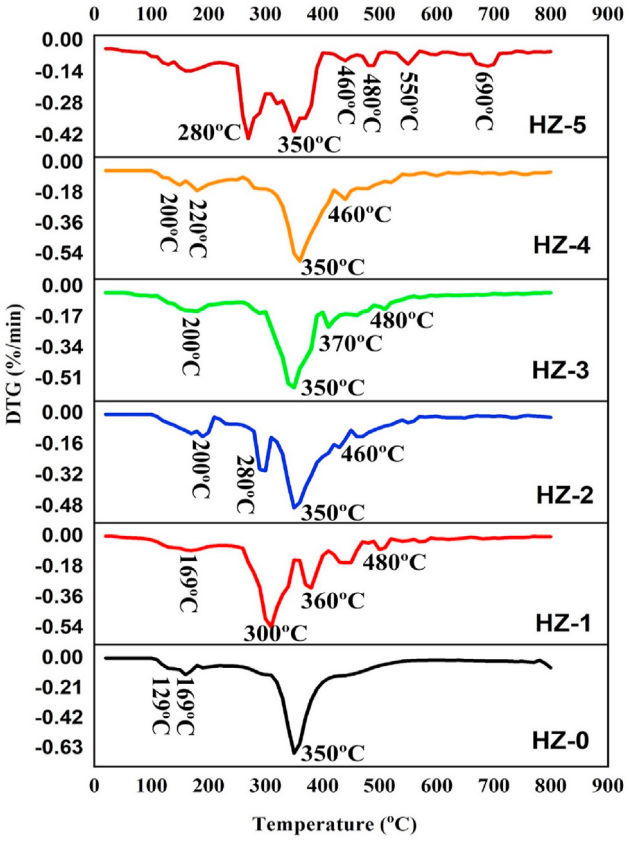

Fig. 10 – DTG curve of HZ0, HZ1, HZ2, HZ3, HZ4, HZ5.

ZrP in the defensive layer of the carbonaceous char and THC helped to develop a network within char to strengthen it.

4.5. *Thermal stability analysis*

The thermal stability of the coated samples was analyzed by the thermogravimetric analysis and the changes in residual mass were recorded versus the temperature. Fig. 9 shows the evolution of the mass of coating samples between room temperature to 800 °C. It provided a good estimate of the residual weight at 800 °C. The final residue mass recorded for

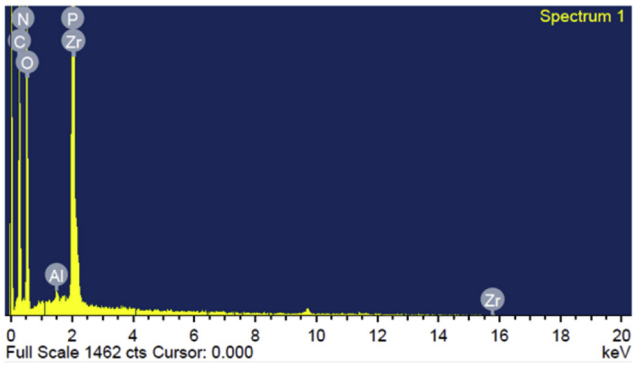

Fig. 12 – EDX of THC and ZrP reinforced intumescent coating.

HZ0, HZ1, HZ2, HZ3, HZ4 and HZ5 was 36%, 36%, 37%, 36%, 36% and 38% respectively. As the maximum char residue was recorded for HZ5. As the percentage of THC used is very small and contribution in terms of residual mass is minimum. For the formulation containing 0.5:0.5 THC and ZrP, approximately 5.5% increase in residual mass was recorded.

However, the addition of fillers was found insignificant in influencing over the final char residue. This is due to the high melting point of silicon and zirconium present in the THC and ZrP compound. It has four stages of degradation named as melting, intumescence, char formation and degradation [43]. Approximately 9–10% mass loss was noticed in between 0 and 220 °C. Boric acid is converted into boron oxide at 147 °C [44] and the dehydration of THC. The major mass loss was observed from 220°C to 460 °C, which accounts for around 45–50%. It consists in the decomposition of other intumescent coating ingredients such as APP, melamine, epoxy and hardener and the evaporation of the physical/chemical absorbed water. The decomposition of epoxy used in this system occurs in the 220–330 °C temperature range [45] whereas, the condensation of the phosphate groups forming zirconium pyrophosphate as an end product takes place between 450 and 600 °C [46]. Major degradation of the control formulation, HZ0 started at 280 °C–420 °C. On the other hand, HZ5 showed improved degradation temperature from 280 °C to 700 °C. This

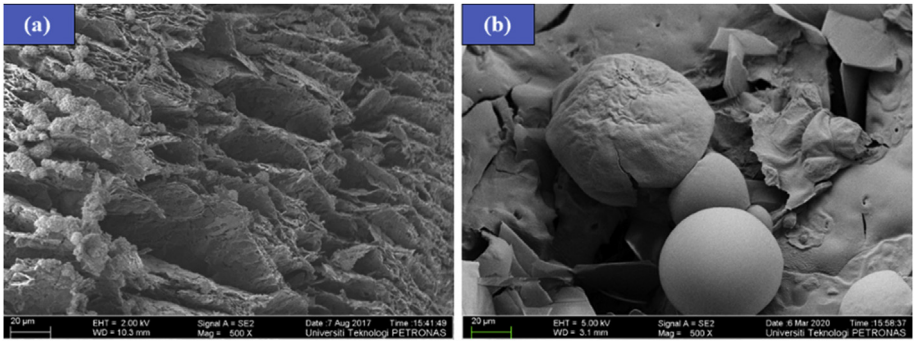

Fig. 11 – FESEM images of (a) sample HZ 0 (b) sample HZ 5 after the fire test.

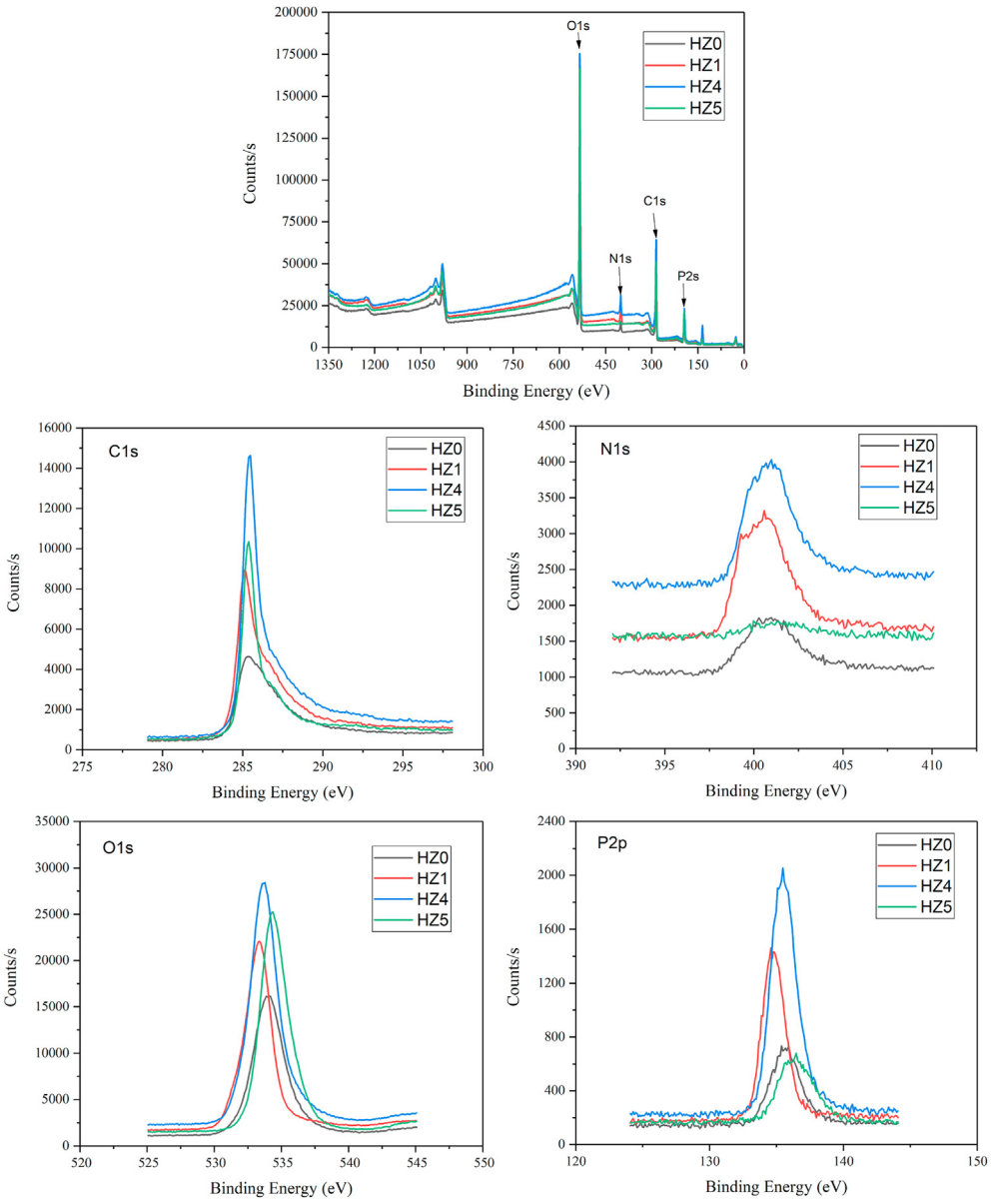

Fig. 13 – XPS Spectra and spectrum of Carbon (C1s), Oxygen (O1s), Phosphorus (P2p), Nitrogen (N1s) for HZ 0, HZ 1, HZ 4, and HZ 5.

was attributed to the appropriate combination of the mass percentage of THC-ZrP.

DTG curve of sample HZ0, HZ1, HZ2, HZ3, HZ4 and HZ5 presented in Fig. 10. All the samples have undergone their first stage of thermal degradation started from 120 °C to 220 °C. Polyamide hardener degrade at 124 °C [22], dehydration process of boric acid took place at 129 °C and meta boric acid was produced and finally meta boric acid converted into boron oxide [47]. However, HZ-5 has shown improved degradation temperature in comparison to the other samples. The second stage of degradation started from 290 °C to 350 °C. Melamine started degrading at 290 °C and APP by 350 °C resulted releasing of N_2 and NH_3 [22]. The third stage degradation was noticed at 460 °C due to the decomposition of epoxy resin and other intumescent coating ingredients. At this point only crystalline boron phosphate is remained in the system and their degradation occurred at approximate 480 °C.

4.6. *FESEM analysis of char*

The char expansion was examined using the furnace fire test and its morphology was studied using FESEM. Fig. 11 (a, b) shows the evidence of cracks on the char surface during coating degradation is shown in Fig. 11 (a) for the reference sample without any filler. The presence of voids and dumps in the char layers offered poor fire performance [48]. The better and clearer surface was obtained with sample HZ-5 in Fig. 11 (c). Pristine ZrP displays a plate-like structure consisting of numerous plate-like agglomerates. In comparison with pristine ZrP, even though the round edge of the sheets indicates

Table 2 – Elemental composition of THC-ZrP reinforced coating system.

Elements	Composition (at. %)					
	HZ 0	HZ 1	HZ 2	HZ 3	HZ 4	HZ 5
N1s	4.21	6.81	2.72	4.65	4.57	0.97
O1s	52.41	45.05	55.55	55.32	45.54	54.41
C1s	39.16	42.64	35.65	36.25	43.45	42.06
P2p	4.22	5.5	6.13	3.77	6.43	2.55

that it is not very crystalline. Moreover, ZrP and THC dimensions range from several microns to sub-micrometer which possibly can help to strengthen the char.

The compact worm-like microstructure was observed in Fig. 11 (c) of HZ5, which is known to provide a better fire shielding at higher temperature [49]. Due to the emission of the gaseous compound during the thermal degradation, bubbles are formed, resulting in micro sized holes and cracks (Fig. 11 (c)). Bubbles formed due to dehydration of epoxy resin, boric acid, and NH_3 gases from the decomposition of melamine, APP and EG [50]. The presence of aluminum and zirconium was confirmed from the EDX analysis (Fig. 12). Despite having voids and cracks in the char, the development of the silicate network is visible and is supportive of forming the individual self-protective over on the char on the exposure to fire [25].

4.7. *XPS analysis of THC and zirconium phosphate reinforced intumescent coating*

To analyze the elemental composition of the char residue, XPS analysis was conducted. The results had been plotted in XPS spectra as shown in Fig. 13. XPS results are summarized in Table 2. Fig. 14 represents the XPS intensity spectrum of O1s, C1s, N1s and P2p. It can be observed that C1s peak is higher for HZ4 and lower for controlled sample. HZ5 is showing the highest peak of O1s. N1s and P2p peak is found higher for HZ4. HZ1, HZ4 and HZ5 showed an improved carbon content as 8.16%, 9.87% and 6.89%, respectively as compared to the reference formulation HZ0. Similarly, reduced oxygen content in the residue char was obtained for HZ1 and HZ4 as 14.04% and 13.10%, respectively while 3.67% O_2 content increased in HZ5. However, phosphorus and nitrogen percentage were improved for HZ4 by 34.3% and 7.8% but found in a lesser extent in HZ5 formulation. This is due to proportion of weight percentage used in this study.

The binding energies of 284 eV and 284.6 eV are ascribed to C = C and C-C graphite-type bonds, respectively, while the 285.2 eV band is assigned to C-N bonding [51]. Due to the inclusion of ZrP in the epoxy-APP-Mel-boric acid char, the peak region of 284 eV is considerably greater than the linked to peak for APP. This result revealed a mechanism that a-ZrP's Brønsted acid spots (H+) for crosslinking, dehydrogenation and dehydration during fire test [34]. The O1s band showed two peaks at roughly 531.7 eV (C-O and P-O respective) and 532.9 eV (PO-P, C-O, and C-O-P respective), signifying the formation of phosphorus crosslinking [52]. The binding energy of 134.2 eV for the P2p spectrum may be correlated with the PO_3 or P-O-C structures developed by phosphorus-rich crosslink [31]. The residue of APP/ZrP indicates the existence of molecular Zr, while the normal Zr 3d doublet (186.2 eV and 183.7 eV) corresponds to the standard Zr (IV) unit [53]. This shows that implementing a-ZrP in the epoxy coating outcomes in high catalytic consequences, that also improves the carbonation and slow downed the heat penetration into the substrate. The spectrum of N 1s is divided into two peaks spectrum, the C-N bond is at 400.6 eV, and the N-H bond is at 402 eV as stated in Fig. 13.

4.8. *Analysis of water resistance of THC-zirconium phosphate reinforced intumescent coating*

Water absorption by the coated samples was measured using the water immersion test according to ASTM D870 standard. The weight of each sample was recorded before and after the water immersion test (Fig. 14). The highest weight change noticed in samples was 0.40%. The steel sample did not gain any weight during the test period, which indicated its corrosion tendency while exposing in water for 14 days. The lowest weight change rate was found for the sample HZ-5 with a value close to 0.02%. Except for the specimen HZ5, all samples

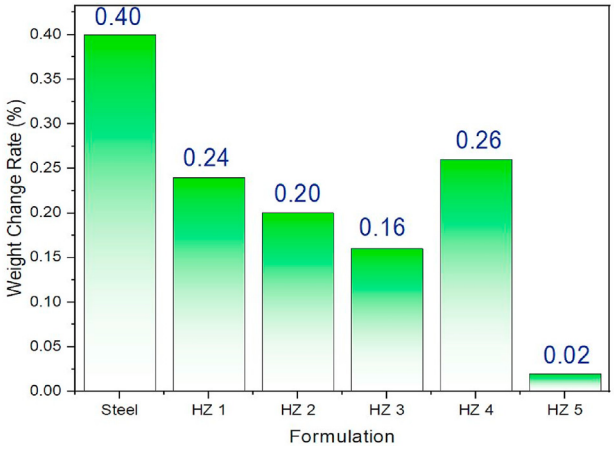

Fig. 14 – Weight change of samples after 14 days of immersion in water.

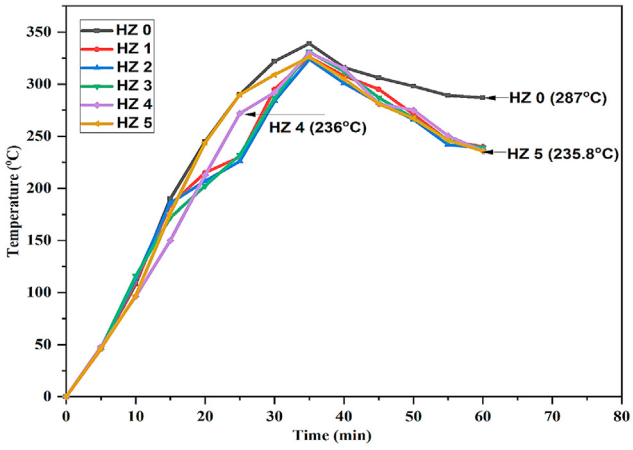

Fig. 15 – Time versus temperature curve for THC-Zirconium Phosphate reinforced intumescent coatings after water immersion test.

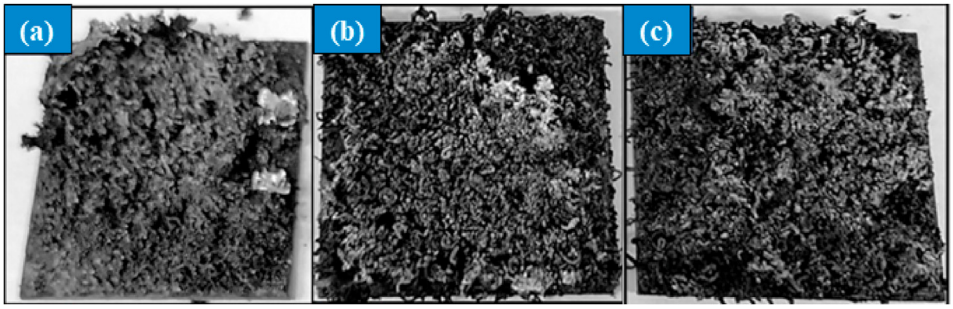

Fig. 16 – Physical Structure of Char After Water immersion test (a) HZ 0 (b) HZ 1 (c) HZ 5.

underwent weight loss after 96 h of immersion in water. Absorption took place in HZ5 until day 9. Water absorption properties seemed better as the amount of THC is increasing other than HZ4, which probably was due to the inappropriate dispersion of the fillers.

In the initial stage, when coatings are immersed in water, the weight without equilibrium continues to increase [54]. Throughout the first 24 h, all the coating samples obtain an extreme weight increase. The second method that contains water immersion coating is the solvation cycle, which is where hydrophilic fire protectives fillers exceed the water and ions permeation method and reduce the overall weight of the coating [55]. For all formulations, weight loss occurred after the 96 h. From literature, this weight loss was the product of the diffusion from the coating and settled in the water with certain hydrophilic flame retardants additives [56,57]. Through the multilayer structure and hydrophobic characteristics of THCs in which water is insoluble, water resistance can thus be concluded with increasing content of ZrP, and THCs fillers improved. This is essential to limit the water absorption of the material surface.

4.9. *Thermal insulation performance of coating after water immersion test*

Aiming to analyze the thermal insulation property of water immersed samples of THC-ZrP reinforced intumescent coating system, fire test, according to ASTM E119 was performed. Temperature with respect to time curve is shown in Fig. 15. The reference sample (HZ-0) have shown the highest backside temperature of 287 °C while approximately 17.8% reduction in temperature was noticed for HZ5 (0.5% of THC and 0.5% of Zirconium Phosphate) which was the lowest among all the formulations tested. The backside substrate temperature for HZ1, HZ2, HZ3, HZ4 and HZ5 was attained 240 °C, 238.6 °C, 239 °C, 236 °C and 235.8 °C respectively. The fire protective performance seemed to have shrunk after the water immersion test. Approximate 5% higher backside substrate temperature was recorded for control formulation, HZ-0, compare to the thermal performance results obtained before the water immersion test. Similarly, the backside substrate temperature for HZ1, HZ2, HZ3, HZ4, and HZ5 was increased around 4.5%, 4.2%, 5.7%, 5.0% and 7.1%, respectively.

4.10. *Physical appearance and char morphology after water immersion test*

The oxidized layer on the surface of the char after furnace fire test of coating samples exposed to water was examined critically. Fig. 16 (a, b, c). An uneven surface of the char was noted for control formulation (HZ0). Detached and fragile char was observed for coating formulations HZ1 and HZ3 after the water immersion test. Micro size holes were present in the

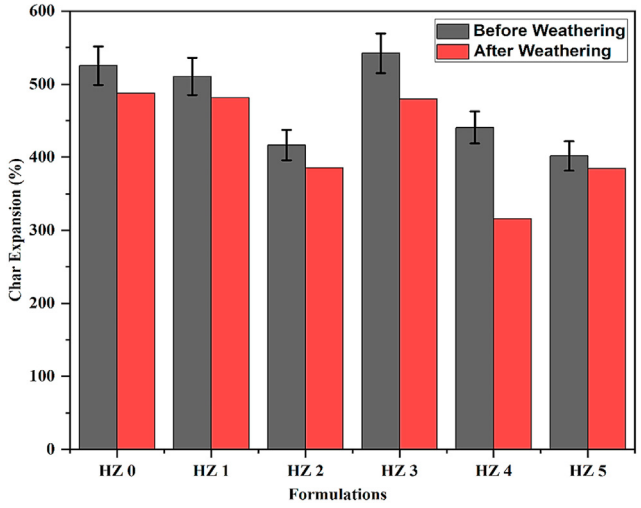

Fig. 17 – Comparison of Char Expansion Before and After water immersion Test.

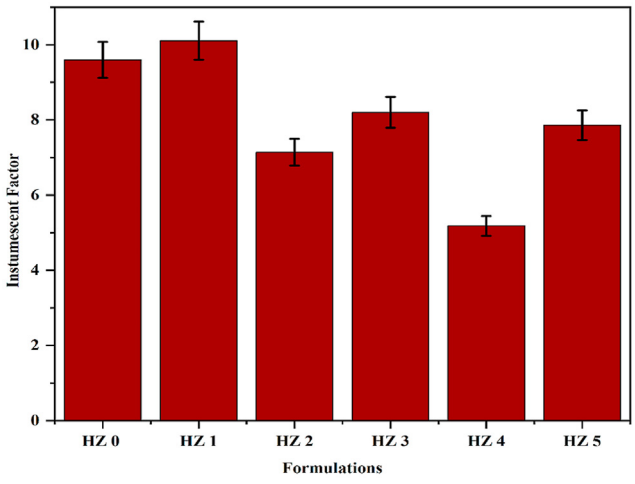

Fig. 18 – Intumescent Factor (IF) calculated for THC reinforced after water immersion test.

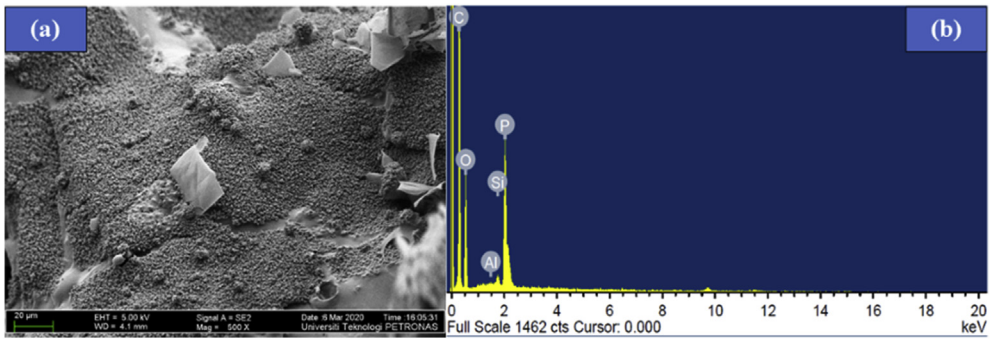

Fig. 19 – (a) FESEM image of HZ 5 after water immersion test (b) EDX of HZ 5 after Water Immersion Test.

formulation HZ2 with uneven structure. A comparatively better char structure was observed for HZ4 and HZ5. No cracks and holes were present in HZ5, and uniform char structure was achieved.

It was concluded that water immersion did not influence on the physical appearance of char after furnace fire test. Char expansion was calculated using the following equation.

$$\text{Char Expansion} = \frac{\textit{Char Thikcness}}{\textit{Coating Thickness}} \quad (3)$$

Char expansion for all the formulations before and after the water immersion test was calculated using the Eq. (3) and presented in Fig. 17. Char expansion seemed to have reduced after the water immersion test. Approximately 7.19% reduction in expansion was recorded for the control formulation, HZ0. Lowest char expansion was noticed for HZ4, which is about 315.8% and 28% less than what it was before immersion. Highest char expansion was noted for HZ1, which is about 481.3%. The slight variation of 4.28% was observed for HZ5, which showed less affects after water immersion test. Intumescent Factor 'I' was also calculated using Eq. (2) similarly for all the formulations referring to Fig. 18 below. Approximately 7.9%, 6.6%, 8.8%, 14.58%, 46.04% and 5.07% decrement in the value was noted for HZ0, HZ1, HZ2, HZ3, H 4 and HZ5 respectively. This is because some of the hydrophilic flame-retardant components are water-soluble and weak some linkage of the polymer binder and decrease the resistance to corrosion and the fire of intumescent coating [58]. Due to higher contents of THCs that could withstand water even after 96 h of water dip, HZ 5 has the minimum decrease in the expansion of the char. There are no hydroxyl groups and active ions on the main or basal surfaces of the THC and ZrP elementary layer that justify hydrophobicity and minimize water absorption through the coating surface. That is because of fire protective materials destabilize the chemical reactivity of the protective layer.

Micrograph after water immersion test of sample HZ5 showing in Fig. 19 (a) is not as similar as it was reported in Fig. 11 (b). Tiny pores were visible around the char surface, and they allowed the penetration of heat to the substrate. Although the presence of fillers was seen, understandably sand-like rough surfaces were visible in the entire char residue due to the water absorption effect before burning the coating. Fig. 19 (b) is the spectrum assuring the presence of Al and Si, which is an essential compound needed to develop silicate network which formed their shielding over the char surfaces to protect the layers from fire exposure.

In the char framework, formulation HZ5, significant cracks and streaky char are found. This was considered due to exposure to the flame-retardant fillers (EG-APP-MEL). APP cannot react with PER or MEL in this way; amine and phosphoric acid will not be successfully sent out by the coating to create a strong "foam" char structure, the coating is, therefore, hard to grow. The EDX results continue to render flakes Al, P and Si due to their hydrophobic features that can increase the intumescent coating's water resistance. This study identified that coating formulation containing 0.5wt% THC and 0.5wt% ZrP showed better char compactness, fire prevention compared to control formulation. The fire performance after the water immersion test of this coating HZ 5 showed approximately 8% increase in substrate temperature which is 235.8 °C and this temperature is far below the critical temperature of steel.

The weather tests indicated that the coating was strengthened with the inclusion of THCs and ZrP. THCs and ZrP layer structure and hydrophobic characteristic the main strategies to improve the water resistance of the coating. G. Wang [26], observed similar behaviour of coating for water resistance when glass flakes were added in an intumescent protective coating, due to its flaky assembly decrease the movement of fire. It was concluded that the intracellular structure of graphite flakes improves water and ion penetration routes via the coating [59]. The structure of such fillers can, therefore, be concluded to boost the water-resistance efficiency of the intumescent layer.

5. Conclusions

This research was aimed to analyze the combination effects of ceramic fillers (THC and zirconium phosphate) on the thermal performance of the intumescent fire-retardant coating, which is successfully achieved. Char structure has been improved for HZ4 and HZ5. Minimum backside substrate temperature achieved 219 °C for the formulation HZ5. FTIR results confirm the presence of C=C, C=O, B-O-P, P-O-P bonds. XRD

reconfirm the existence of sassolite. Zirconium phosphate is also detected in the XRD spectrum of char. The higher char residue among the studied formulations is the formulation HZ5 at around 38%. FESEM analysis shows the improved char layer for HZ5, having less cracks and voids as compared to the controlled formulation. Presence of silicate network over the char residue also confirmed from the micrographs. Improved carbon content was seen in HZ1, HZ4 and HZ5 by 8.16%, 9.87% and 6.89%, respectively in comparison to the control sample. Water immersion test discover HZ5 has better resistance to water absorption since it has shown only 0.02% weight change in 14 days. HZ4 has shown a relatively higher weight change of 0.26%. Laboratory scale jet fire test conducted after the immersion test reveal the control formulation shows 287 °C after 1 h of fire exposure, and approximately 17.83% temperature reduction is recorded for HZ5.

Declaration of Competing Interest

The authors declare that they have no known competing financial interests or personal relationships that could have appeared to influence the work reported in this paper.

Acknowledgements

The research was financially supported under the Minister of Higher Education (MOHE), Grant No. FRGS/1/2019/TK05/UTP/01/1 under FRGS Scheme. Authors also acknowledge the laboratory support of Advanced and Functional Materials, Corrosion Research Centre, Universiti Teknologi PETRONAS, Malaysia.

REFERENCES

[1] Duquesne S, Magnet S, Jama C, Delobel R. Intumescent paints: fire protective coatings for metallic substrates. Surf Coating Technol 2004;180:302–7.
[2] Bourbigot S, Le Bras M, Duquesne S, Rochery M. Recent advances for intumescent polymers. Macromol Mater Eng 2004;289(6):499–511.
[3] Horrocks A, Kandola BK, Davies P, Zhang S, Padbury S. Developments in flame retardant textiles–a review. Polym Degrad Stabil 2005;88(1):3–12.
[4] Wladyka-Przybylak M, Kozlowski R. The thermal characteristics of different intumescent coatings. Fire Mater 1999;23(1):33–43.
[5] Duquesne S, Bachelet P, Bellayer S, Bourbigot S, Mertens W. Influence of inorganic fillers on the fire protection of intumescent coatings. J Fire Sci 2013;31(3):258–75.
[6] Jimenez M, Duquesne S, Bourbigot S. Intumescent fire protective coating: toward a better understanding of their mechanism of action. Thermochim Acta 2006;449(1–2):16–26.
[7] Gardelle B, Duquesne S, Rerat V, Bourbigot S. Thermal degradation and fire performance of intumescent silicone-based coatings. Polym Adv Technol 2013;24(1):62–9.
[8] Li G, Liang G, He T, Yang Q, Song X. Effects of EG and MoSi2 on thermal degradation of intumescent coating. Polym Degrad Stabil 2007;92(4):569–79.
[9] Li G, Yang J, He T, Wu Y, Liang G. An investigation of the thermal degradation of the intumescent coating containing MoO3 and Fe2O3. Surf Coating Technol 2008;202(13):3121–8.
[10] Hull TR, Witkowski A, Hollingbery L. Fire Retardant action of mineral fillers. Polym Degrad Stabil 2011;96:1462–9.
[11] Lu H, Wilkie CA. The influence of α-zirconium phosphate on fire performance of EVA and PS composites. Polym Adv Technol 2011;22:1123–30.
[12] Xing W, Zhang P, Song L, Wang X, Hu Y. Effects of alpha-zirconium phosphate on thermal degradation and flame retardancy of transparent intumescent fire protective coating. Mater Res Bull 2014;49:1–6.
[13] Luo Y, Xie D, Chen Y, Han T, Chen R, Sheng X, et al. Synergistic effect of ammonium polyphosphate and α-zirconium phosphate in flame-retardant poly(vinyl alcohol) aerogels. Polym Degrad Stabil 2019;170:109019.
[14] Kashiwagi T, Gilman JW, Butler KM, Harris RH, Shields JR, Asano A. Flame retardant mechanism of silca gel/silica. Fire Mater 2000;24:277–89.
[15] Yu ZL, Yang N, Apostolopoulou-Kalkavoura V, Qin B, Ma ZH, Xing WY, et al. Fire-retardant and thermally insulating phenolic-silica aerogels. Angew Chem Int Ed 2017;27:4538–42.
[16] Kuilla T, Bhadra S, Yao D, Kim NH, Bose S, Lee JH. Recent advances in graphene based polymer composites. Prog Polym Sci 2010;35:1350–75.
[17] Wilson I, Keeling J. Global occurrence, geology and characteristics of tubular halloysite deposits. Clay Miner 2016;51(3):309–24.
[18] Lecouvet B, Sclavons M, Balilly C, Bourbigot S. A comprehensive study of the synergistic flame retardant mechanisms of halloysite in intumescent polypropylene. Polym Degrad Stabil 2013;98(11):2268–81.
[19] Gaaz TS, Sulong AB, Kadhum AAH, Al-Amiery AA, Nassir MH, Jaaz AH. The impact of halloysite on the thermo-mechanical properties of polymer composites. Molecules 2017;22:838.
[20] Gillani QF, Ahmad F, Mutalib A, Ibrahim M, Syahera E. Thermal degradation and char morphology of HTCs reinforced epoxy based intumescent fire retardant coatings, Key Engineering Materials. Trans Tech Publ; 2016. p. 83–8.
[21] Alongi J, Frache A. Flame retardancy properties of α-zirconium phosphate based composites. Polym Degrad Stabil 2010;95(9):1928–33.
[22] Ullah S, Ahmad F, Yusoff PSMM. Effect of boric acid and melamine on the intumescent fire-retardant coating composition for the fire protection of structural steel substrates. J Appl Polym Sci 2013;128(5):2983–93.
[23] Jimenez M, Duquesne S, Bourbigot S. Multiscale experimental approach for developing high-performance intumescent coatings. Ind Eng Chem Res 2006;45(13):4500–8.
[24] Tanomaru Filho M, Leonardo MR, Bonifacio KC, Dametto FR, Silva IAB. The use of ultrasound for cleaning the surface of stainless steel and nickel-titanium endodontic instruments. Int Endod J 2001;34:581–5.
[25] Dzulkafli HH, Ahmad F, Ullah S, Hussain P, Mamat O, Megat-Yusoff PSM. Effects of talc on fire retarding, thermal degradation and water resistance of intumescent coating. Appl Clay Sci 2017;146:350–61.
[26] Wang G, Yang J. Influences of glass flakes on fire protection and water resistance of waterborne intumescent fire resistive coating for steel structure. Prog Org Coating 2011;70(2–3):150–6.
[27] Deng J, Wang YC, Zhao JP, Shi H. Pyrolysis kinetics of ZrP-containing aliphatic waterborne polyurethane-based intumescent coating for flame-retarding plywood. Prog Org Coating 2020;147:105845.

[28] Ullah S, Ahmad F, Shariff AM, Bustam MA. Synergistic effects of kaolin clay on intumescent fire retardant coating composition for fire protection of structural steel substrate. Polym Degrad Stabil 2014;110:91–103. 0.
[29] Shao Z-B, Deng C, Tan Y, Chen M-J, Chen L, Wang Y-Z. An efficient mono-component polymeric intumescent flame retardant for polypropylene: preparation and application. ACS Appl Mater Interfaces 2014;6(10):7363–70.
[30] Ullah S, Ahmad F. Effects of zirconium silicate reinforcement on expandable graphite based intumescent fire retardant coating. Polym Degrad Stabil 2014;103:49–62.
[31] Zhao C-X, Liu Y, Wang D-Y, Wang D-L, Wang Y-Z. Synergistic effect of ammonium polyphosphate and layered double hydroxide on flame retardant properties of poly (vinyl alcohol). Polym Degrad Stabil 2008;93(7):1323–31.
[32] Yasir M, Amir N, Ahmad F, Ullah S, Jimenez M. Effect of basalt fibers dispersion on steel fire protection performance of epoxy-based intumescent coatings. Prog Org Coating 2018;122:229–38.
[33] Liu Y, Chen L, Wang T, Xu Y, Zhang Q, Ma L, et al. Direct conversion of cellulose into C 6 alditols over Ru/C combined with H+-released boron phosphate in an aqueous phase. RSC Adv 2014;4(94):52402–9.
[34] Liu XQ, Wang DY, Wang XL, Chen L, Wang YZ. Synthesis of organo-modified α-zirconium phosphate and its effect on the flame retardancy of IFR poly(lactic acid) systems. Polym Degrad Stabil 2011;96(55):771–7.
[35] Medvedev E, Komarevskaya AS. IR spectroscopic study of the phase composition of boric acid as a component of glass batch. Glass Ceram 2007;64(1–2):42–6.
[36] Mahapatra SS, Karak N. s-Triazine containing flame retardant hyperbranched polyamines: synthesis, characterization and properties evaluation. Polym Degrad Stabil 2007;92(6):947–55.
[37] Puri RG, Khanna A. Effect of cenospheres on the char formation and fire protective performance of water-based intumescent coatings on structural steel. Prog Org Coating 2016;92:8–15.
[38] Feng C, Liang M, Chen W, Huang J, Liu H. Flame retardancy and thermal degradation of intumescent flame retardant EVA composite with efficient charring agent. J Anal Appl Pyrol 2015;113:266–73.
[39] Rodríguez JA, Hanson JC, Chupas PJ. In-situ characterization of heterogeneous catalysts. Wiley Online Library; 2013.
[40] Vyas P, Chaudhuri RG, Gopalakrishnan G, Baladhandapani M. Development of novel formulation for high performance fire retardant cementitious mortars. Mater Today Proc 2020;28:1245–53.
[41] Li H, Hu Z, Zhang S, Gu X, Wang H, Jiang P, et al. Effects of titanium dioxide on the flammability and char formation of water-based coatings containing intumescent flame retardants. Prog Org Coating 2015;78:318–24.
[42] Fu X-L, Wang X, Xing W, Zhang P, Song L, Hu Y. Two-dimensional cardanol-derived zirconium phosphate hybrid as flame retardant and smoke suppressant for epoxy resin. Polym Degrad Stabil 2018;151:172–80.
[43] Griffin GJ, Bicknell AD, Brown TJ. Studies on the effect of atmospheric oxygen content on the thermal resistance of intumescent, fire-retardant coatings. J Fire Sci 2005;23(4):303–28.
[44] Ullah S, Ahmad F, Shariff A,M, Bustam MA, Gonda G, Gillani QF. Effects of ammonium polyphosphate and boric acid on the thermal degradation of an intumescent fire retardant coating. Prog Org Coating 2017;109:70–82.
[45] Yasir M, Ahmad F, Megat-Yusoff PS, Ullah S, Jimenez M. Quantifying the effects of basalt fibers on thermal degradation and fire performance of epoxy-based intumescent coating for fire protection of steel substrate. Prog Org Coating 2019;132:148–58.
[46] Cai G, Lu H, Xu S, Wang Z, Wilkie CA. Fire properties od silylated α-zirconium phosphate composites based on polystyrene. Polym Adv Technol 2013;24:646–52.
[47] Cinausero N, Howell B, Schmaucks G, Marosi G, Brzozwski Z, Cuesta JL, et al. Fire retardancy of polymers: new strategies and mechanisms. Royal Society of Chemistry; 2008.
[48] Tsai K-C. Influence of substrate on fire performance of wall lining materials. Construct Build Mater 2009;23(10):3258–63.
[49] Mohamad WF, Ahmad F, Ullah S. Effect of inorganic fillers on thermal performance and char morphology of intumescent fire retardant coating. Asian J Sci Res 2013;6(2):263–71.
[50] Yao M, Wu H, Liu H, Zhou Z, Wang T, Jiao Y, et al. In-situ growth of boron nitride for the effect of layer-by-layer assembly modified magnesium hydroxide on flame retardancy, smoke suppression, toxicity and char formation in EVA. Polym Degrad Stabil 2021;183:109417.
[51] Li W, Tang X-Z, Zhang H-B, Jiang Z-G, Yu Z-Z, Du X-S, et al. Simultaneous surface functionalization and reduction of graphene oxide with octadecylamine for electrically conductive polystyrene composites. Carbon 2011;49(14):4724–30.
[52] Yuan B, Fan A, Yang M, Chen X, Hu Y, Bao C, et al. The effects of graphene on the flammability and fire behavior of intumescent flame retardant polypropylene composites at different flame scenarios. Polym Degrad Stabil 2017;143:42–56.
[53] Ardizzone S, Bianchi C. XPS characterization of sulphated zirconia catalysts: the role of iron. Surf Interface Anal 2000;30(1):77–80. An International Journal devoted to the development and application of techniques for the analysis of surfaces, interfaces and thin films.
[54] Hazwani Dzulkafli H, Ahmad F, Ullah S, Hussain P, Mamat O, Megat-Yusoff PSM. Effects of talc on fire retarding, thermal degradation and water resistance of intumescent coating. Appl Clay Sci 2017;146(Supplement C):350–61.
[55] de la Fuente D, Bohm M, Houyoux C, Rohwerder M, Morcillo M. The settling of critical levels of soluble salts for painting. Prog Org Coating 2007;58(1):23–32.
[56] Zhang N, Zhang M, Zhang J, Guo X, Wang H, Niu B, et al. Flexible water-resistant intumescent coatings: fabrication, characterization, and fire protective performance. Prog Org Coating 2019;137:105322.
[57] Wang J, Wang G. Influences of montmorillonite on fire protection, water and corrosion resistance of waterborne intumescent fire retardant coating for steel structure. Surf Coating Technol 2014;239:177–84.
[58] Yew M, Sulong NR, Yew M, Amalina M, Johan M. Eggshells: a novel bio-filler for intumescent flame-retardant coatings. Prog Org Coating 2015;81:116–24.
[59] Luo W, Li Y, Zou H, Liang M. Study of different-sized sulfur-free expandable graphite on morphology and properties of water-blown semi-rigid polyurethane foams. RSC Adv 2014;4(70):37302–10.